OPTIMAL PRECONDITIONING FOR THE COUPLING OF ADAPTIVE FINITE AND BOUNDARY ELEMENTS

MICHAEL FEISCHL[*], THOMAS FÜHRER[*], DIRK PRAETORIUS[*] AND ERNST P. STEPHAN[†]

[*] Institute for Analysis and Scientific Computing
Vienna University of Technology
Wiedner Hauptstrasse 8–10, 1040 Vienna, Austria
e-mail: {michael.feischl,thomas.fuehrer,dirk.praetorius}@tuwien.ac.at

[†]Insitute for Applied Mathematics
Leibniz University Hannover
Welfengarten 1, 30167 Hannover, Germany
e-mail: stephan@ifam.uni-hannover.de

Key words: FEM-BEM coupling, preconditioner, additive Schwarz, adaptivity

Abstract. We consider the adaptive coupling of finite element method (FEM) and boundary element (BEM) in 2D. It is well-known that the condition number of the Galerkin matrix depends on the minimal diameter of the elements in the triangulation and therefore can grow severely if the triangulation is locally refined. Usually, this affects the solver, i.e., the number of iterations used by an iterative solver can be arbitrarily large. Thus, the construction of an optimal preconditioner is a necessary task to ensure performance as well as reliable results. Here, optimality is understood in the sense that the condition number of the preconditioned system remains bounded independently of the (minimal and maximal) diameter as well as the number of elements.

In our talk, we present some block-diagonal preconditioner for the non-symmetric Johnson-Nédélec FEM-BEM coupling on locally refined triangulations. The diagonal blocks correspond to local additive Schwarz preconditioners for either the FEM part or the BEM part. We report on the optimality result for this preconditioning from [5] and underline this mathematical result by numerical experiments.
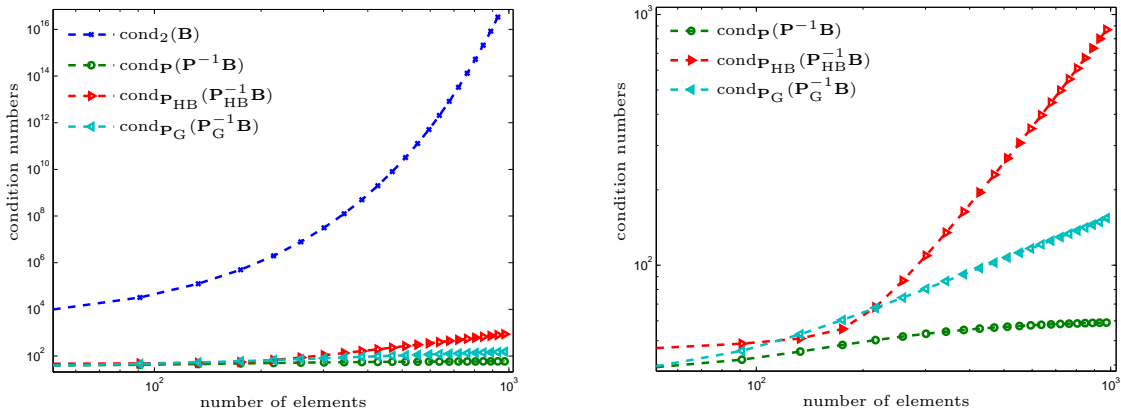

Figure 1: Experimental growth of the ℓ^2-condition number of the unpreconditioned matrix $\mathbf{B}$ (blue) and the condition numbers $\mathrm{cond}_{\mathbf{P}}(\mathbf{P}^{-1}\mathbf{B})$ (green) as well as $\mathrm{cond}_{\mathbf{P}_{\mathrm{HB}}}(\mathbf{P}_{\mathrm{HB}}^{-1}\mathbf{B})$ (red) and $\mathrm{cond}_{\mathbf{P}_{\mathrm{G}}}(\mathbf{P}_{\mathrm{G}}^{-1}\mathbf{B})$ (turquois) on a sequence of strongly adapted meshes. See Section 6 for a detailed description.

1 INTRODUCTION

The coupling of FEM and BEM is the natural method of choice for the numerical treatment of certain partial differential equations (PDEs) on unbounded computational domains, e.g., full-space problems arising in electrostatics or magnetostatics. The overall problem is split into a problem in a bounded domain Ω and an exterior problem in $\mathbb{R}^2 \backslash \overline{\Omega}$ which is reformulated by an integral equation on the boundary $\Gamma = \partial\Omega$. As far as conforming methods with direct integral formulation of the exterior problem are concerned, essentially two types of coupling methods have been thoroughly analyzed: While the mathematical literature mainly studied the symmetric coupling from [3], stability of the Johnson-Nédélec coupling [7] for polygonal coupling boundaries has only been proved recently [10, 11, 1]. Since the Johnson-Nédélec coupling involves only two boundary integral operators and avoids, in particular, the use of the hypersingular integral operator, it is often preferred in practice.

For a Laplace-type transmission problem (see Section 3 for details), the Johnson-Nédélec coupling reads as follows: Find (u, ϕ) such that

$$\langle A\nabla u\,,\,\nabla v\rangle_\Omega - \langle \phi\,,\,v\rangle_\Gamma = \langle f\,,\,v\rangle_\Omega + \langle \phi_0\,,\,v\rangle_\Gamma, \tag{1a}$$

$$\langle \psi\,,\,(\tfrac{1}{2} - \mathcal{K})u + \mathcal{V}\phi\rangle_\Gamma = \langle \psi\,,\,(\tfrac{1}{2} - \mathcal{K})u_0\rangle_\Gamma, \tag{1b}$$

for all test functions (v, ψ). The material behavior is described by A, and $\mathcal{V}$ resp. $\mathcal{K}$ are the simple-layer resp. double-layer integral operators, see Section 3 below for proper definitions.

Using linear FEM in Ω to discretize u and piecewise constants on Γ to discretize the flux ϕ, (1) becomes a linear system of equations

2

$$\mathbf{Bu} = \mathbf{f} \quad \text{with block matrix} \quad \mathbf{B} = \begin{pmatrix} \mathbf{A} & -\mathbf{M}^T \\ \frac{1}{2}\mathbf{M} - \mathbf{K} & \mathbf{V} \end{pmatrix} + \mathbf{ss}^T, \tag{2}$$

where $\mathbf{s}$ denotes an appropriate stabilization vector which ensures positivity of $\mathbf{B}$ (see Lemma 1).

Adaptive methods — for FEM and BEM — resolve singularities of given data and solutions and are known to be optimal in the sense that the error decreases with the best possible algebraic rate [4]. Therefore, adaptive methods can lower the computational costs dramatically. However, a main drawback of adaptive FEM and BEM, hence also of the adaptive FEM-BEM coupling, is that the condition number of the corresponding matrices hinges on the minimal diameter of the elements and thus becomes bad on adaptively refined triangulations, see Figure 1 for the growth of the condition number of the unpreconditioned FEM-BEM matrix $\mathbf{B}$. It is therefore a necessary task to construct *optimal*, i.e. mesh-independent, preconditioners in order to preserve the advantages of the adaptive method.

In [5], we propose and thoroughly analyze a block-diagonal preconditioner

$$\mathbf{P} = \begin{pmatrix} \mathbf{P}_A & \mathbf{0} \\ \mathbf{0} & \mathbf{P}_\mathcal{V} \end{pmatrix} \tag{3}$$

for the FEM-BEM matrix $\mathbf{B}$. Roughly speaking, $\mathbf{P}_A$ corresponds to a preconditioner for the FEM part and $\mathbf{P}_\mathcal{V}$ to a preconditioner for the BEM part of (2). It is reasonable to use the whole hierarchy of the adaptively generated meshes to construct so-called multilevel methods. Here, we consider local additive Schwarz preconditioners for both blocks $\mathbf{P}_A$ and $\mathbf{P}_\mathcal{V}$, which correspond to a diagonal scaling on local subsets of degrees of freedom (nodes). These subsets contain the newly created nodes and their immediate neighbours, i.e., those regions which are affected by the refinement. As it turns out mathematically (Theorem 4) and practically (Figure 1), the condition number of the preconditioned system $\mathbf{P}^{-1}\mathbf{B}$ is bounded independently of the (local) mesh-size and the number of elements.

Alternatively, one could consider a hierarchical basis preconditioner $\mathbf{P}_{\mathrm{HB}}$, where diagonal scaling is done only on newly created nodes, or a global multilevel preconditioner $\mathbf{P}_{\mathrm{G}}$, where diagonal scaling is done on all nodes. However, we stress that these strategies lead to condition numbers which depend on the sequence of adaptively refined triangulations and are thus sub-optimal, see Figure 1 for an experimental proof.

The outline of this work is as follows: In Section 2, we write down the PDE model problem, which is equivalently reformulated by the Johnson-Nédélec coupling in Section 3. Section 4 deals with the triangulations and ansatz-/test-spaces. The main result about the block-diagonal preconditioning is stated in Section 5, together with the preconditioned GMRES algorithm. Further numerical experiments are given in Section 6. We conclude with some notes on possible extensions and future work (Section 7).

2 PDE FORMULATION OF MODEL PROBLEM

Let $\Omega \subset \mathbb{R}^2$ be a simply connected, bounded Lipschitz domain with polygonal boundary $\Gamma = \partial\Omega$. We consider the following linear transmission problem with given data f, u_0, ϕ_0 and sought solution u, u^{ext}

$$-\operatorname{div}(A\nabla u) = f \qquad \text{in } \Omega, \tag{4a}$$

$$-\Delta u^{\text{ext}} = 0 \qquad \text{in } \mathbb{R}^2\backslash\overline{\Omega}, \tag{4b}$$

$$u - u^{\text{ext}} = u_0 \qquad \text{on } \Gamma, \tag{4c}$$

$$(A\nabla u - \nabla u^{\text{ext}}) \cdot \boldsymbol{n} = \phi_0 \qquad \text{on } \Gamma, \tag{4d}$$

$$u^{\text{ext}}(x) = \mathcal{O}(1/|x|) \qquad \text{as } |x| \to \infty, \tag{4e}$$

where $\boldsymbol{n}$ is the normal vector pointing from Ω to $\mathbb{R}^2\backslash\overline{\Omega}$.

As usual, we denote by $L^2(\Omega)$ the space of square-integrable functions on Ω, and $\langle f, g \rangle_\Omega = \int_\Omega fg\,dx$ denotes the corresponding L^2-scalar product with induced norm $\|f\|^2_{L^2(\Omega)} := \langle f, f \rangle_\Omega$. Analogously, we define $L^2(\Gamma)$, $\langle \cdot, \cdot \rangle_\Gamma$, and $\|\cdot\|_{L^2(\Gamma)}$ for square-integrable functions on the boundary. Moreover, $H^1(\Omega)$ is the Sobolev space for which $u \in H^1(\Omega)$ satisfies $\|u\|_{H^1(\Omega)} := \|u\|^2_{L^2(\Omega)} + \|\nabla u\|^2_{L^2(\Omega)} < \infty$. Let γ_0 denote the trace operator with $\gamma_0 u = u|_\Gamma$ for smooth functions u. It can be extended to $H^1(\Omega)$ functions, where $H^{1/2}(\Gamma) := \gamma_0(H^1(\Omega))$ is again a Hilbert space with dual space $H^{-1/2}(\Gamma) := (H^{1/2}(\Gamma))^*$. Here, duality is understood with respect to the (continuously) extended scalar product $\langle \cdot, \cdot \rangle_\Gamma$. If there is no ambiguity, we write u instead of $\gamma_0 u$ for functions $u \in H^1(\Omega)$.

Let $A \in L^\infty(\Omega)^{2\times 2}$ with $A(x) \in \mathbb{R}^{2\times 2}_{\text{sym}}$ for almost all $x \in \Omega$ denote an operator, used to model the material behavior in the computational domain Ω. We assume that the minimal and maximal eigenvalues of A are bounded in the sense that

$$0 < c_A := \operatorname*{ess\,inf}_{x\in\Omega} \lambda_{\min}(A(x)) \leq C_A := \operatorname*{ess\,sup}_{x\in\Omega} \lambda_{\max}(A(x)) < \infty.$$

Then, the problem (4) is known to admit a unique solution, if we impose the compatibility condition

$$\langle f, 1 \rangle_\Omega + \langle \phi_0, 1 \rangle_\Gamma = 0$$

to ensure the right behavior (4e) in the exterior domain.

3 JOHNSON-NÉDÉLEC COUPLING

We give a short sketch for the derivation of the Johnson-Nédélec coupling. Multiplying (4a) with a test-function v and using Green's first identity, we obtain

$$\langle A\nabla u, \nabla v \rangle_\Omega - \langle A\nabla u \cdot \boldsymbol{n}, v \rangle_\Gamma = \langle f, v \rangle_\Omega.$$

Define $\phi := \frac{\partial u^{\text{ext}}}{\partial \boldsymbol{n}}$. By inserting the jump (4d) of the fluxes, we end up with the first coupling equation (1a).

Green's third formula provides the representation

$$u^{\mathrm{ext}}(x) = \frac{1}{2\pi} \int_\Gamma \frac{(x-y)\cdot \boldsymbol{n}(y)}{|x-y|^2} u^{\mathrm{ext}}(y)\, d\Gamma_y + \frac{1}{2\pi} \int_\Gamma \log|x-y| \frac{\partial u^{\mathrm{ext}}}{\partial \boldsymbol{n}}\, d\Gamma_y, \quad x \in \mathbb{R}^2 \backslash \overline{\Omega}.$$

Restricting this equation to Γ and using the jump (4c), we get

$$u - u_0 = (\tfrac{1}{2} + \mathcal{K})(u - u_0) - \mathcal{V}\phi \quad \text{on } \Gamma, \tag{5}$$

where the linear and continuous boundary integral operators

$$\mathcal{V} : H^{-1/2}(\Gamma) \to H^{1/2}(\Gamma), \qquad \mathcal{K} : H^{1/2}(\Gamma) \to H^{1/2}(\Gamma),$$

formally read

$$\mathcal{V}\phi(x) := -\frac{1}{2\pi} \int_\Gamma \log|x-y|\phi(y)\, d\Gamma_y, \qquad \mathcal{K}v(x) := \frac{1}{2\pi} \int_\Gamma \frac{(x-y)\cdot \boldsymbol{n}(y)}{|x-y|^2} v(y)\, d\Gamma_y.$$

The second coupling equation (1b) is then obtained by testing (5) in $H^{-1/2}(\Gamma)$.

Since the work [10] it is known, that the coupling (1) is stable even on polygonal interfaces for $A(x)$ being the $d \times d$ identity matrix. The work [9] employs an *explicit* stabilization and proves well-posedness if A satisfies $c_A > c_\mathcal{K}/4$, where $c_\mathcal{K} \in [1/2, 1)$ denotes the contraction constant of the double-layer integral operator $\mathcal{K}$, cf. [12]. However, we follow an alternative approach from [1], which ensures the same stability results as in [9, 10, 11], but in contrast to [9, 11] avoids the computation of additional boundary integral equations. We summarize the results of the above mentioned works in the following lemma.

Lemma 1 *Suppose $c_A > c_\mathcal{K}/4$. Define the (stabilized) coupling operator $\mathcal{B} : \mathcal{H} \to \mathcal{H}^*$ by*

$$\langle \mathcal{B}(u, \phi), (v, \psi) \rangle := \langle A\nabla u, \nabla v \rangle_\Omega - \langle \phi, v \rangle_\Gamma + \langle \psi, (\tfrac{1}{2} - \mathcal{K})u + \mathcal{V}\phi \rangle_\Gamma$$
$$+ \langle 1, (\tfrac{1}{2} - \mathcal{K})u + \mathcal{V}\phi \rangle_\Gamma \langle 1, (\tfrac{1}{2} - \mathcal{K})v + \mathcal{V}\psi \rangle_\Gamma$$

and the right-hand side $F \in \mathcal{H}^*$ by

$$F(v, \psi) := \langle f, v \rangle_\Omega + \langle \phi_0, v \rangle_\Gamma + \langle \psi, (\tfrac{1}{2} - \mathcal{K})u_0 \rangle_\Gamma + \langle 1, (\tfrac{1}{2} - \mathcal{K})u_0 \rangle_\Gamma \langle 1, (\tfrac{1}{2} - \mathcal{K})v + \mathcal{V}\psi \rangle_\Gamma$$

for all $(u, \phi), (v, \psi) \in \mathcal{H} = H^1(\Omega) \times H^{-1/2}(\Gamma)$. Let $\mathcal{H}^\ell$ denote an arbitrary closed subspace of $\mathcal{H}$ with $(0, 1) \in \mathcal{H}^\ell$. Then, $(u, \phi) \in \mathcal{H}^\ell$ solves

$$\langle \mathcal{B}(u, \phi), (v, \psi) \rangle = F(v, \psi) \quad \text{for all } (v, \psi) \in \mathcal{H}^\ell \tag{6}$$

if and only if it solves (1). Moreover, $\mathcal{B}$ is positive definite and bounded, i.e.

$$c_\mathcal{B} \|(u, \phi)\|_\mathcal{H}^2 \le \langle \mathcal{B}(u, \phi), (u, \phi) \rangle \le C_\mathcal{B} \|(u, \phi)\|_\mathcal{H}^2 \quad \text{for all } (u, \phi) \in \mathcal{H}.$$

In particular, (6) and thus also (1) admit a unique solution $(u^\ell, \phi^\ell) \in \mathcal{H}^\ell$. ∎

We assume that Ω is scaled in such a way that ellipticity of $\mathcal{V}$ is ensured.
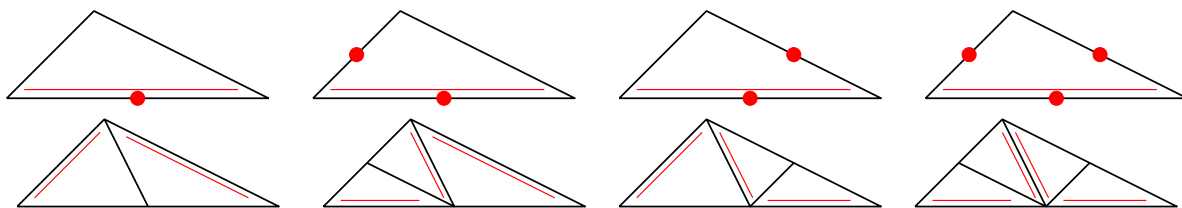
Figure 2: For each triangle $T \in \mathcal{T}_\ell^\Omega$, there is one fixed *reference edge*, indicated by the double line (left, top). Refinement of T is done by bisecting the reference edge, where its midpoint becomes a new node. The reference edges of the son triangles are opposite to this newest vertex (left, bottom). To avoid hanging nodes, one proceeds as follows: We assume that certain edges of T, but at least the reference edge, are marked for refinement (top). Using iterated newest vertex bisection, the element is then split into 2, 3, or 4 son triangles (bottom).

4 MESH-REFINEMENT AND DISCRETIZATION

Let $\mathcal{T}_0^\Omega$ denote a conforming (initial) triangulation of Ω. We stress that $\mathcal{T}_0^\Gamma = \mathcal{T}_0^\Omega|_\Gamma$ is also a conforming triangulation of the boundary Γ. The triangulation $\mathcal{T}_\ell^\Omega$ is obtained from $\mathcal{T}_{\ell-1}^\Omega$ by refining (at least) all marked elements. As refinement strategy, we use the newest vertex bisection (NVB) algorithm, see [8] and references therein as well as Figure 2. The advantage of this strategy is that it, firstly, preserves γ-shape-regularity

$$\sup_{T \in \mathcal{T}_\ell^\Omega} \frac{\mathrm{diam}(T)^2}{|T|} \leq \gamma < \infty$$

for an ℓ-independent $\gamma > 0$ and, secondly, is used to prove optimality of the adaptive FEM-BEM coupling [4]. Here, $\mathrm{diam}(T)$ stands for the diameter and $|T|$ for the area of the triangle T. Note, that $\mathcal{T}_\ell^\Gamma := \mathcal{T}_\ell^\Omega$ defines a conforming triangulation of Γ.

We consider the lowest-order discretizations, i.e. we use the ansatz and test spaces

$$\mathcal{X}^\ell := \{v \in C(\overline{\Omega}) \,:\, v|_T \text{ is affine for all } T \in \mathcal{T}_\ell^\Omega\},$$
$$\mathcal{Y}^\ell := \{\psi \in L^2(\Gamma) \,:\, \psi_T \text{ is constant for all } T \in \mathcal{T}_\ell^\Gamma\}.$$

Let $\mathcal{N}_\ell^\Omega$ resp. $\mathcal{N}_\ell^\Gamma$ denote the set of nodes in the triangulation $\mathcal{T}_\ell^\Omega$ resp. $\mathcal{T}_\ell^\Gamma$. The usual basis of $\mathcal{X}^\ell$ is given by the hat-functions (nodal functions) η_z^ℓ, which satisfy $\eta_z^\ell(z) = 1$ and $\eta_z^\ell(z') = 0$ for $z \neq z'$ and $z, z' \in \mathcal{N}_\ell^\Omega$. Moreover, $\eta_z^\ell|_\Gamma$ gives us a basis for the trace space $\mathcal{X}^\ell|_\Gamma$. The canonical basis of $\mathcal{Y}^\ell$ is given by the characteristic functions χ_T on the element $T \in \mathcal{T}_\ell^\Gamma$. Furthermore, note that the triangulations $(\mathcal{T}_0^\Omega, \mathcal{T}_0^\Gamma), \ldots, (\mathcal{T}_L^\Omega, \mathcal{T}_L^\Gamma)$ provide a nested sequence of subspaces $\mathcal{X}^{\ell-1} \times \mathcal{Y}^{\ell-1} \subseteq \mathcal{X}^\ell \times \mathcal{Y}^\ell$.

To tackle the local nature of adaptive methods in the preconditioner, we define local sets of degrees of freedom

$$\widetilde{\mathcal{N}}_0^X := \mathcal{N}_0^X, \qquad \widetilde{\mathcal{N}}_\ell^X := \mathcal{N}_\ell^X \backslash \mathcal{N}_{\ell-1}^X \cup \{z \in \mathcal{N}_{\ell-1}^X \,:\, \eta_z^\ell \neq \eta_z^{\ell-1}\},$$

where $X = \Omega$ resp. $X = \Gamma$. A visualization is given in Figure 3.
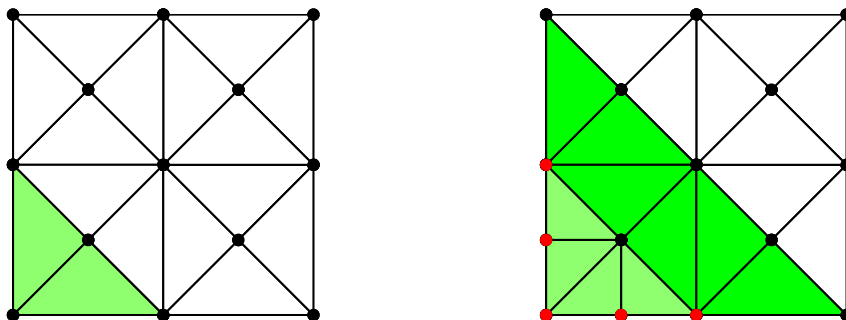
6

Figure 3: The left figure shows a FEM mesh $\mathcal{T}_{\ell-1}^\Omega$, where the two elements (green) are marked for refinement. Bisection of these two elements provides the mesh $\mathcal{T}_\ell^\Omega$ (right), where two *new nodes* are created. The set $\widetilde{\mathcal{N}}_\ell^\Omega$ consists of these new nodes plus their *immediate neighbours* (red), where the corresponding hat-functions have changed.

The discretization of the operator $\mathcal{B}$ from Lemma 1 with respect to the finite dimensional space $\mathcal{X}^L \times \mathcal{Y}^L$ leads to the matrix $\mathbf{B}$ with the block structure as given in (2), where $\mathbf{A}$ corresponds to the discretization of A, $\mathbf{M}$ is a mass-matrix and $\mathbf{K}$ resp. $\mathbf{V}$ correspond to the discretizations of the boundary integral operators $\mathcal{K}$ resp. $\mathcal{V}$. Moreover, $\mathbf{ss}^T$ denotes the rank-1 stabilization term of the operator $\mathcal{B}$. Also note that positivity of $\mathbf{B}$ is inherited from $\mathcal{B}$.

5 BLOCK-DIAGONAL PRECONDITIONER

Throughout, we analyze the symmetric and positive definite block-diagonal preconditioner (3), with $\mathbf{P}_A$ being a "good" approximation of the matrix $\mathbf{A} + \mathbf{s}'\mathbf{s}'^T$, where $\mathbf{s}'\mathbf{s}'^T$ is the block of the stabilization matrix $\mathbf{ss}^T$ that corresponds to the degrees of freedom in $\mathcal{X}^L$, and $\mathbf{P}_\mathcal{V}$ being a "good" approximation of the matrix $\mathbf{V}$. In mathematical terms, this is expressed by *spectral equivalence*, i.e. there exist constants $d_A, D_A, d_\mathcal{V}, D_\mathcal{V} > 0$ such that

$$d_A \mathbf{x}^T \mathbf{P}_A \mathbf{x} \leq \mathbf{x}^T \mathbf{A} \mathbf{x} \leq D_A \mathbf{x}^T \mathbf{P}_A \mathbf{x} \tag{7}$$

$$d_\mathcal{V} \mathbf{y}^T \mathbf{P}_\mathcal{V} \mathbf{y} \leq \mathbf{y}^T \mathbf{V} \mathbf{y} \leq D_\mathcal{V} \mathbf{y}^T \mathbf{P}_\mathcal{V} \mathbf{y}. \tag{8}$$

for all $\mathbf{x} \in \mathbb{R}^{N_L}$, $\mathbf{y} \in \mathbb{R}^{M_L}$. We speak of *optimal* preconditioners if these constants are independent of the diameters of the elements, the number of elements in $\mathcal{T}_L^\Omega$ resp. $\mathcal{T}_L^\Gamma$ and the level L.

Altogether, we seek for a solution $\mathbf{u}$ of

$$\mathbf{P}^{-1} \mathbf{B} \mathbf{u} = \mathbf{P}^{-1} \mathbf{f}. \tag{9}$$

5.1 Preconditioned GMRES algorithm

We consider the GMRES algorithm to solve (9), where we replace the usual euclidean inner product with the inner product induced by the symmetric and positive definite

matrix $\mathbf{P}$, i.e. $\mathbf{y}^T\mathbf{x}$ is replaced by $\mathbf{y}^T\mathbf{P}\mathbf{x}$. The algorithm stops, if the residual $\mathbf{r}^j$ in the j-th step of the algorithm satisfies $\|\mathbf{r}^j\|_{\mathbf{P}} \leq \tau\|\mathbf{r}^0\|_{\mathbf{P}}$ for some given tolerance parameter $0 < \tau < 1$. Here, $\mathbf{r}^0 = \mathbf{P}^{-1}(\mathbf{B}\mathbf{u}^0 - \mathbf{f})$ denotes the initial residual with initial guess $\mathbf{u}_0$. It can be proven, that there holds the following reduction of the j-th residual generated by the preconditioned GMRES algorithm

$$\|\mathbf{r}^j\|_{\mathbf{P}} \leq (1 - \alpha^2/\beta^2)^{j/2}\|\mathbf{r}^0\|_{\mathbf{P}},$$

where $\| \cdot \|_{\mathbf{P}}$ denotes the norm induced by $\mathbf{P}$. The constants α, β depend on $\mathbf{P}^{-1}\mathbf{B}$ and are estimated in the proof of the main result (Theorem 4 below). We stress, that the preconditioned GMRES algorithm with inner product induced by $\mathbf{P}$ can be implemented without explicit knowledge of $\mathbf{P}$. This is advantageous in practice, since only $\mathbf{P}^{-1}$ is known. We refer to [5] for details.

5.2 Main result

Let $\mathbf{I}^\ell$ denote the matrix which realizes the canonical embedding $\widetilde{\mathcal{X}}^\ell = \mathrm{span}\{\eta_z^\ell \,:\, z \in \widetilde{\mathcal{N}}_\ell^\Omega\} \to \mathcal{X}^L$ and let $\mathbf{D}_\Omega^\ell$ denote the diagonal of the matrix $\mathbf{A} + \mathbf{s}'\mathbf{s}'^T$ (with respect to $\mathcal{X}^\ell$) restricted to the degrees of freedom in $\widetilde{\mathcal{N}}_\ell^\Omega$. Our local multilevel preconditioner is defined by

$$\mathbf{P}_A^{-1} := \sum_{\ell=0}^{L} \mathbf{I}^\ell(\mathbf{D}_\Omega^\ell)^{-1}(\mathbf{I}^\ell)^T.$$

A proof of the following theorem follows from the analysis of [14] and the references therein.

Theorem 2 *The constants d_A, D_A in the spectral equivalence estimate* (7) *depend only on Ω, A, and the initial triangulation $\mathcal{T}_0^\Omega$.* ■

The construction of $\mathbf{P}_\mathcal{V}^{-1}$ is a little bit more involved. Let $\chi_z^\ell := (\eta_z^\ell|_\Gamma)'$ denote the Haar basis function. Note that

$$\widetilde{\mathcal{Y}}^\ell := \mathrm{span}\{\chi_z^\ell \,:\, z \in \widetilde{\mathcal{N}}_\ell^\Gamma\} \subsetneq \mathcal{Y}^\ell.$$

Let $\mathbf{H}^\ell$ denote a matrix representation of the Haar basis functions in $\widetilde{\mathcal{Y}}^\ell$ with respect to the canonical basis of $\mathcal{Y}^\ell$. Moreover, let $\mathbf{D}_\Gamma^\ell$ be the diagonal of the matrix $(\mathbf{H}^\ell)^T\mathbf{V}\mathbf{H}^\ell$ and let $\mathbf{J}^\ell$ be the matrix realization of the canonical embedding $\mathcal{Y}^\ell \to \mathcal{Y}^L$. Our local multilevel preconditioner reads

$$\mathbf{P}_\mathcal{V}^{-1} := \mathbf{1}\langle 1\,,\, \mathcal{V}1\rangle_\Gamma\mathbf{1}^T + \sum_{\ell=0}^{L} \mathbf{J}^\ell\mathbf{H}^\ell(\mathbf{D}_\Gamma^\ell)^{-1}(\mathbf{H}^\ell)^T(\mathbf{J}^\ell)^T,$$

where $\mathbf{1}$ denotes a vector whose entries are all 1. Optimality of $\mathbf{P}_\mathcal{V}$ follows from the optimality of a multilevel additive Schwarz preconditioner for the hypersingular integral operator analyzed in [6].

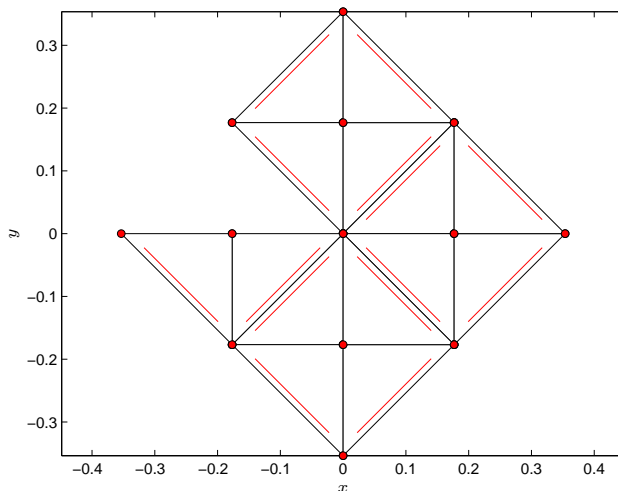**Figure 4**: Z-shaped domain Ω with $\mathrm{diam}(\Omega) < 1$ and initial volume triangulation $\mathcal{T}_0^\Omega$. The initial triangulation $\mathcal{T}_0^\Gamma$ of the boundary is given by the restriction $\mathcal{T}_0^\Omega|_\Gamma$ of the volume triangulation on the boundary. The initial triangulations consist of $\#\mathcal{T}_0^\Omega = 14$ resp. $\#\mathcal{T}_0^\Gamma = 10$ elements. Red lines indicate the reference edges for the newest vertex bisection of the initial volume triangulation.

Theorem 3 *The constants $d_\mathcal{V}, D_\mathcal{V}$ in the spectral equivalence estimate* (8) *depend only on Γ and the initial triangulation $\mathcal{T}_0^\Gamma$.* ∎

By $\mathrm{cond}_\mathbf{P}(\mathbf{B}) = \|\mathbf{B}\|_\mathbf{P}\|\mathbf{B}^{-1}\|_\mathbf{P}$, we denote the condition number of $\mathbf{B}$ with respect to the matrix norm induced by the symmetric and positive definite matrix $\mathbf{P}$.

Theorem 4 *Theorem 2 and 3 imply that the condition number*

$$\mathrm{cond}_\mathbf{P}(\mathbf{P}^{-1}\mathbf{B}) \leq C < \infty$$

is uniformly bounded. Moreover, the j-th residual from the preconditioned GMRES algorithm satisfies

$$\|\mathbf{r}^j\|_\mathbf{P} \leq q^j\|\mathbf{r}^0\|_\mathbf{P}.$$

The constants $C > 0$, $0 < q < 1$ depend only on Ω, A, and the initial triangulation $\mathcal{T}_0^\Omega$. ∎

6   NUMERICAL EXAMPLES

Let Ω denote the Z-shaped domain sketched in Figure 4. We consider the coupling problem with $A(x)$ being the 2×2 identity matrix. Hence, $\mathrm{div}(A\nabla u) = \Delta u$. We prescribe the exact solutions
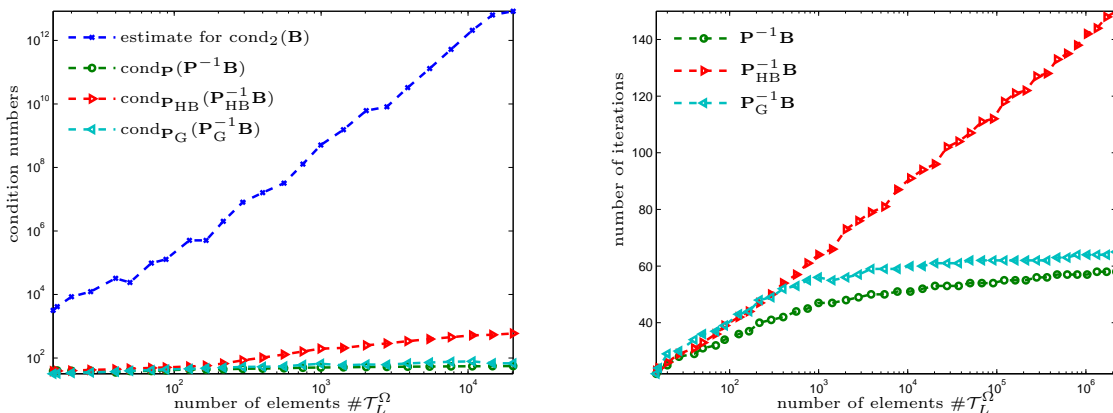
9

Figure 5: We compare the different types of preconditioners $\mathbf{P}$, $\mathbf{P}_{\mathrm{HB}}$ and $\mathbf{P}_{\mathrm{G}}$. Left: Experimental condition numbers for $\mathbf{B}$ and the preconditioned systems $\mathbf{P}^{-1}\mathbf{B}$, $\mathbf{P}_{\mathrm{HB}}^{-1}\mathbf{B}$, and $\mathbf{P}_{\mathrm{G}}^{-1}\mathbf{B}$ for the example of Section 6. Right: Number of iterations for solving the Johnson-Nédélec coupling using the preconditioned GMRES algorithm from Section 5.1 with tolerance $\tau = 10^{-6}$ and inner product induced by $\mathbf{P}$ resp. $\mathbf{P}_{\mathrm{HB}}$ resp. $\mathbf{P}_{\mathrm{G}}$ on adaptively refined meshes. We choose $\mathbf{u}_0 = \mathbf{0}$ for the initial guess.

$$u(x,y) = r^{4/7}\cos(4\theta/7) \qquad \text{for } (x,y) \in \Omega,$$

$$u^{\mathrm{ext}}(x,y) = \frac{1}{10}\frac{x+y-\frac{1}{8}}{(x-\frac{1}{8})^2+y^2} \quad \text{for } (x,y) \in \mathbb{R}^2\backslash\overline{\Omega},$$

where (r,θ) denote the 2D polar coordinates. The data $f \in L^2(\Omega)$, $u_0 \in H^{1/2}(\Gamma)$, and $\phi_0 \in H^{-1/2}(\Gamma)$ are computed thereof. We stress that u exhibits a generic singularity at the reentrant corner $(0,0) \in \mathbb{R}^2$. To steer the mesh-adaptivity, we use the residual-based error estimator from [1] which dates back to [2] for the symmetric coupling.

In Figure 5 we plot the condition numbers of the matrices $\mathbf{B}$, $\mathbf{P}^{-1}\mathbf{B}$. For comparison we consider two other preconditioners: On the one hand a hierarchical basis preconditioner $\mathbf{P}_{\mathrm{HB}}$ which is defined as $\mathbf{P}$, but the local subsets $\widetilde{\mathcal{N}}_\ell^X$ are replaced by $\mathcal{N}_\ell^X\backslash\mathcal{N}_{\ell-1}^X$ for $X = \Omega,\Gamma$, i.e. diagonal scaling is done only on newly created nodes. On the other hand a global multilevel preconditioner $\mathbf{P}_{\mathrm{G}}$, where $\widetilde{\mathcal{N}}_\ell^X$ is replaced by $\mathcal{N}_\ell^X$, i.e. diagonal scaling is done on all nodes in the triangulation.

Next, we count the number of iterations j used in the preconditioned GMRES algorithm to reduce the relative residual $\|\mathbf{r}^j\|_{\mathbf{P}}/\|\mathbf{r}^0\|_{\mathbf{P}}$ by a factor of $\tau = 10^{-6}$. We set $\mathbf{u}_0 = \mathbf{0}$ as the initial guess. For comparison we also count the number of iterations when using $\mathbf{P}_{\mathrm{HB}}$ or $\mathbf{P}_{\mathrm{G}}$ instead of $\mathbf{P}$. The results are visualized in Figure 5.

Finally, we consider an artificial refinement of the Z-shape given in Figure 4, where we mark only those elements for refinement which are closest to the origin $(0,0)$. This will lead to strongly adapted triangulations. In Figure 1, the condition numbers of $\mathbf{B}$,

$\mathbf{P}^{-1}\mathbf{B}$, $\mathbf{P}_{\mathrm{HB}}^{-1}\mathbf{B}$, and $\mathbf{P}_{\mathrm{G}}^{-1}\mathbf{B}$ are given. We obtain optimality of $\mathbf{P}^{-1}$, whereas $\mathbf{P}_{\mathrm{HB}}$ and $\mathbf{P}_{\mathrm{G}}$ are sub-optimal.

7 EXTENSION AND OUTLOOK

We have seen that the proposed block-diagonal preconditioner $\mathbf{P}$ from (3) for the (adaptive) Johnson-Nédélec coupling is optimal. For the symmetric coupling, $\mathbf{P}$ defines also an optimal preconditioner, leading to the same results as in Theorem 4.

Moreover, for 3D problems, similar block-diagonal preconditioners can be used, provided that the blocks $\mathbf{P}_A$, $\mathbf{P}_{\mathcal{V}}$ satisfy the spectral equivalence estimates (7)–(8) with constants independent of mesh-related quantities. We stress that optimal local multi-level preconditioners $\mathbf{P}_A$ for the FEM part can be constructed in 3D, see, e.g., [13] and the references therein, whereas — to the best of the author's knowledge — it is still an open problem to construct an optimal preconditioner $\mathbf{P}_{\mathcal{V}}$ for the BEM part (simple-layer integral operator) on adaptively refined triangulations.

REFERENCES

[1] Aurada, M., Feischl, M., Führer, T., Karkulik, M., Melenk, J.M. and Praetorius, D. Classical FEM-BEM coupling methods: non-linearities, well-posedness, and adaptivity. *Comput. Mech.* (2013) **51**:399–419.

[2] Carstensen, C. and Stephan, E.P. Adaptive coupling of boundary and finite elements. *RAIRO Modél. Math. Anal. Numér.* (1995) **29**:779–817.

[3] Costabel, M. A symmetric method for the coupling of finite elements and boundary elements. In *The mathematics of finite elements and applications, VI* (1988) Academic Press London, 281–288.

[4] Feischl, M., Führer, T. and Praetorius, D. Adaptive FEM, BEM, and FEM-BEM coupling with optimal rates for strongly non-symmetric problems. *ASC Report, Vienna University of Technology* (2013) **39/2013**.

[5] Feischl, M., Führer, T., Praetorius, D. and Stephan, E.P. Optimal preconditioning for the symmetric and non-symmetric coupling of adaptive finite elements and boundary elements. *ASC Report, Vienna University of Technology* (2013) **36/2013**.

[6] Feischl, M., Führer, T., Praetorius, D. and Stephan, E.P. Efficient additive Schwarz preconditioning for hypersingular integral equations. *ASC Report, Vienna University of Technology* (2013) **25/2013**.

[7] Johnson, C. and Nédélec, J.C. On the coupling of boundary integral and finite element methods. *Math. Comp.* (1980) **35**:1063–1079.

[8] Karkulik, M., Pavlicek, D. and Praetorius, D. On 2D newest vertex bisection: Optimality of mesh-closure and H^1-stability of L_2-projection. *Constr. Approx.* (2013) **38**:213–234.

[9] Of, G. and Steinbach, O. Is the one-equation coupling of finite and boundary element methods always stable? *Z. Angew. Math. Mech.* (2013) **93**:476–484.

[10] Sayas, F.J. The validity of Johnson-Nédélec's BEM-FEM coupling on polygonal interfaces. *SIAM J. Numer. Anal.* (2009) **47**:3451–3463.

[11] Steinbach, O. A note on the stable one-equation coupling of finite and boundary elements. *SIAM J. Numer. Anal.* (2011) **49**:1521–1531.

[12] Steinbach, O. and Wendland, W.L. On C. Neumann's method for second-order elliptic systems in domains with non-smooth boundaries. *J. Math. Anal. Appl.* (2001) **262**:733–748.

[13] Xu, J., Chen, L. and Nochetto, R.H. Optimal multilevel methods for $H(\text{grad})$, $H(\text{curl})$, and $H(\text{div})$ systems on graded and unstructured grids. In *Multiscale, nonlinear and adaptive approximation* (2009) Springer, 599–659.

[14] Xu, X., Chen, H. and Hoppe, R.H.W. Optimality of local multilevel methods on adaptively refined meshes for elliptic boundary value problems. *J. Numer. Math.* (2010) **18**:59–90.